



Contents lists available at ScienceDirect

Bioorganic & Medicinal Chemistry

journal homepage: www.elsevier.com/locate/bmc

Synthesis and biological evaluation of 6*H*-pyrido[2',1':2,3]imidazo[4,5-*c*]isoquinolin-5(6*H*)-ones as antimitotic agents and inhibitors of tubulin polymerization



Tao Meng^{a,†}, Wei Wang^{b,†}, Zhixiang Zhang^b, Lanping Ma^{a,*}, Yongliang Zhang^a, Zehong Miao^{b,*}, Jingkang Shen^{a,*}

^a Division of Medicinal Chemistry, State Key Laboratory of Drug Research, Shanghai Institute of Materia Medica, Chinese Academy of Sciences, Shanghai 201203, People's Republic of China

^b Division of Antitumor Pharmacology, State Key Laboratory of Drug Research, Shanghai Institute of Materia Medica, Chinese Academy of Sciences, Shanghai 201203, People's Republic of China

ARTICLE INFO

Article history:

Received 19 August 2013

Revised 20 October 2013

Accepted 3 December 2013

Available online 11 December 2013

Keywords:

6*H*-Pyrido[2',1':2,3]imidazo[4,5-*c*]isoquinolin-5(6*H*)-ones

Antitumor agents

Inhibitors of tubulin polymerization

Colchicine binding site

ABSTRACT

A series of 6*H*-pyrido[2',1':2,3]imidazo[4,5-*c*]isoquinolin-5(6*H*)-ones have been synthesized and evaluated for their antiproliferative activities. Among them, compounds **2j** and **4d** displayed potent cytotoxic activities in vitro against HeLa cell line with IC₅₀ values of 0.07 and 0.06 μM, respectively. In general, the antiproliferative activities are correlated with the inhibitory effect on tubulin polymerization and binding property of the colchicine binding site. In addition, flow cytometry and immunofluorescence analysis revealed selected compounds caused G2/M phase arrest of the cell cycle and disruption of the mitotic spindle assembly, which had correlation with proliferation inhibitory activity.

© 2014 Published by Elsevier Ltd.

1. Introduction

Attacking the microtubule system is a common strategy to inhibit tumor cell proliferation. The microtubule constituted by α,β-tubulin heterodimers, is regarded as one of the most important targets to treat many types of malignancies.^{1–3} A still expanding family of antimitotic drugs displaying a wide structural heterogeneity has been identified to act on tubulin, and they usually bind to tubulin at three distinct sites: the taxane site, the vinca site and the colchicine site.^{4,5}

A large number of structurally diverse antimitotic agents have been identified as inhibitors of the polymerization of tubulin (e.g., vinblastine and vincristine) and stabilizers of the microtubule structure (e.g., paclitaxel and docetaxel), which are widely used clinically as important chemotherapeutic drugs for the treatment of many malignancies.^{6,7} Colchicine is another significant antimitotic agent, played an important role in the elucidation of the properties and functions of tubulin and microtubules. However, it has not been applied in anticancer therapy due to its narrow therapeutic

window. In the past few years, small molecular colchicines site binders based on combretastatin A4 were actively pursued as antimitotic agents which exerted potent cytotoxic activities.⁸ However, up until now, no representative members of this class have been employed as cancer chemotherapeutic agents in the market. Therefore, great efforts have recently been made to develop novel small-molecular tubulin binders derived not only from natural sources but also by screening compound libraries in combination with traditional medicinal chemistry, such as ABT-751, BNC105, ELR510444 and IRC-083927 showed good efficacy.^{9–12}

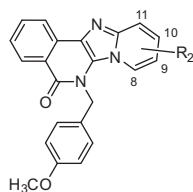
We have earlier described a series of 6*H*-pyrido[2',1':2,3]imidazo[4,5-*c*]isoquinolin-5(6*H*)-ones-derived tubulin polymerization inhibitors with in vitro antitumor activity, which was generated by using a three-component reaction.¹³ One of the compounds, MT-7 (**1a**, Table 1), exhibited cytotoxic activity in the cell based screen, with an averaged IC₅₀ of 2.58 μM ranging from 0.85 to 5.01 μM.^{13,14} More importantly, MT-7 was found to be able to induce cell cycle arrest at G2/M phase. Continuing our search strategy for novel potent tubulin-targeting compounds, we conducted further investigation on the structural parameters of 6*H*-pyrido[2',1':2,3]imidazo[4,5-*c*]isoquinolin-5(6*H*)-one derivatives associated with their antiproliferative activity. Some of them demonstrated the antiproliferative ability against HeLa cell line. Moreover, **4d** inhibited the growth of various tumor cell lines.¹⁵

* Corresponding authors. Tel.: +86 21 50806600/5407; fax: +86 21 50807088.

E-mail addresses: lpma@simmm.ac.cn (L. Ma), zhm@jding.dhs.org (Z. Miao), jkshen@simmm.ac.cn (J. Shen).

† These authors contributed equally to this work.

Table 1
Antiproliferative activity of **1a–f** against HeLa cells



Compd	R ₂ substitution	HeLa IC ₅₀ (μM) ^a
1a (MT-7)	H	1.8 ^{13,14}
1b	9-CH ₃	6.6 ¹³
1c	8-CH ₃	>10
1d	11-CH ₃	>10
1e	8-CH ₃ , 9-Br	>10
1f	9-Br, 10-CH ₃	>10

^a IC₅₀ values are mean ± SD from three independent tests.

We also found that these analogues exerted the antiproliferative function by arresting tumor cells at mitosis and inhibition of tubulin polymerization. Antitubulin activities of the most active compounds were comparable to the compound vincristine (VCR) and colchicine (COL). This study also helps us to dissect the structure–activity relationship of this antimetabolic library and will guide our ongoing research.

2. Results and discussion

2.1. Chemistry

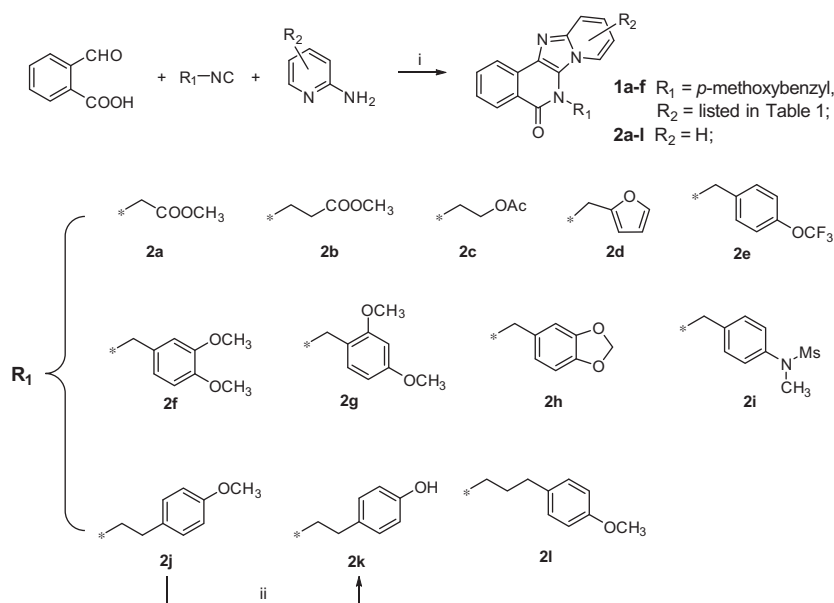
The general method used for the synthesis of the 6*H*-pyrido[2',1':2,3]imidazo[4,5-*c*]isoquinolin-5(6*H*)-one derivatives **1a–f** and **2a–l** is depicted in Scheme 1 as reported previously by our group.¹³ The preparation of 6*H*-pyrido[2',1':2,3]imidazo[4,5-*c*]isoquinolin-5(6*H*)-ones (compounds **1a–f**, **2a–j**, **2l** and intermediate **3**) were readily achieved by three component condensation of various commercial or synthetic isocyanides, 2-aminopyridines and phthaldehydic acid. The compound **2j** was demethylated

with a solution of BBr₃ in CH₂Cl₂ to afford the phenolic compound **2k**. Derivatives **4a–h** were synthesized by microwave reaction of the bromo derivative **3** with corresponding amines in the presence of CuI, L-proline and K₂CO₃ in DMSO at 150 °C while irradiating at 250 W for 30 min (Scheme 2).

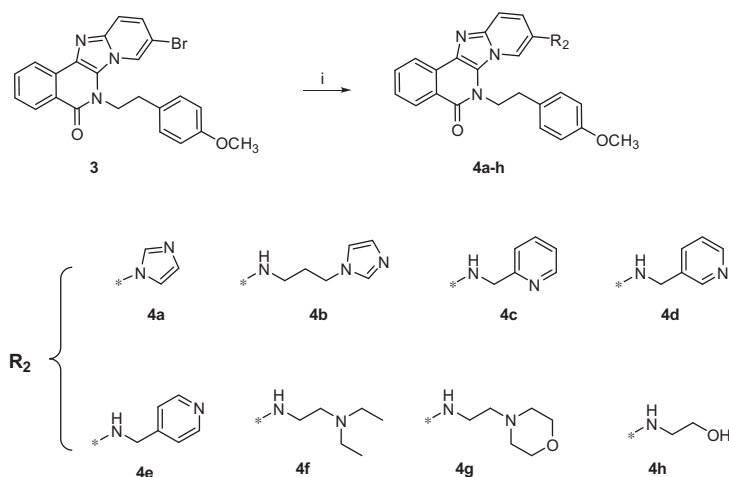
2.1.1. In vitro antiproliferative activity assays

The compounds' antiproliferative activities were evaluated in vitro against the HeLa cell line (Tables 1 and 2). The preliminary SAR information in Table 1 of various R₂ substitutions showed that only compounds **1b** out of five compounds (**1b–f**) exerted IC₅₀ of 6.6 μM (Table 1), which indicated that modifications at C-9 position might be tolerated compare to positions 8, 10 or 11. The antiproliferative activity was closely related to the 4-methoxybenzyl at R₁ group according to our previous SAR studies,¹³ which could suggest the existence of the H-bonding interaction with the amino acid side chains of the putative biological target. Thus various functional groups containing H-bond acceptors were introduced by reaction with the corresponding isocyanides (**2a–l**, Table 2). Analysis of the substitution pattern indicated that the presence of *para*-methoxy group at phenyl ring was essential to the bioactivity. The replacement of the methoxy group of **1a** by the 4-trifluoromethoxy (**2e**) or *N*-methylmethanesulfonamide (**2i**) resulted with the complete loss of activity. 3,4-Dimethoxy substitution at phenyl ring produced inactive derivative **2f**, while 2,4-dimethoxy substitution gave derivative (**2g**) with fair activity (IC₅₀ = 2.2 μM), whereas cleavage of the ether groups (**2k**) resulted in loss of potency. The aliphatic esters (**2a–c**) and furanmethyl substitution (**2d**) were also completely inactive. Noteworthy, the dependence of antiproliferative activity upon spacer length between phenyl ring and the rest of the molecule is crucial, increasing the number of methylene units to two resulted in a 25-fold increase of activity (**2j** vs MT-7). Further chain elongation led to loss of activity in antiproliferative activity (**2l**).

Encouraged by further SARs of R₁ group, keeping the preferred 2-(4-methoxyphenyl)ethyl unchanged, attention shifted to exploration of the 9-position of the molecule **2j**. Furthermore, we tried to increase the water solubility of the highly lipophilic parent compounds by the introduction of hydrophilic side chains (entries **4a–h**, Scheme 2). As expected, this region of the molecule allows various structural modifications with diverse hydrophilic



Scheme 1. Reagents and conditions: (i) MeOH, 55 °C, overnight; (ii) BBr₃, dry CH₂Cl₂, –78 to –25 °C;



Scheme 2. Reagents and conditions: (i) CuI, L-proline, K₂CO₃, DMSO, μ W (150 °C, 250 W), 30 min.

Table 2
Antiproliferative activity of **2a–l** and **4a–h** against HeLa cells

Compd	HeLa IC ₅₀ (μM) ^a
2a	>10
2b	>10
2c	>10
2d	>10
2e	>10
2f	>10
2g	2.24 ± 0.57
2h	>10
2i	>10
2j	0.07 ± 0.01
2k	>10
2l	>10
4a	0.12 ± 0.01
4b	0.77 ± 0.20
4c	0.24 ± 0.12
4d	0.06 ± 0.01
4e	0.10 ± 0.02
4f	2.28 ± 0.33
4g	1.20 ± 0.62
4h	0.35 ± 0.08
VCR	0.015 ± 0.003

^a IC₅₀ values are mean ± SD from three independent tests.

nitrogen-contained heterocyclic ring systems such as imidazole (**4a**, **4b**), pyridine (**4c–e**), morpholine (**4g**) or polar substitution group as *N,N*-diethylethanediamine (**4f**) and ethanolamine (**4h**). In comparison with the parent compound **2j**, by introduction of the hydrophilic substitutions, compounds **4a–h** showed moderate to potent antiproliferative activity. Among those, the 3-picolylamino substitution (**4d**) displayed strong antiproliferative activity (IC₅₀ HeLa: 0.06 μM), and it was the most active compound in this assay. Similar activity was found for the constitutional isomers **4c** and **4e** (IC₅₀ HeLa: 0.24 and 0.10 μM, respectively). In addition, the imidazole (**4a**, **4b**) and ethanolamine (**4h**) substituted analogues also showed activities in the submicromolar range, with IC₅₀ values ranging from 0.12 to 0.77 μM. Analysis of the above SAR results attracted our interest for further studies on their mechanisms of action.

2.2. Cell-cycle progression analysis

When entering the mitosis phase, cells are tuning round and then split into two daughter cells. In light of the observations with

microscopes, we found that HeLa cells became round after the treatment of compounds **2a–l** and **4a–h**. Naturally, we speculated that the antiproliferative activities of these compounds were related to the interference with cell cycle progression.¹⁶ Based on their antiproliferative activity in vitro, **2j** and **4d** were selected as the representative compounds to analyse the effect on cell cycle profile in HeLa cells. Cells were cultured for 12 h in the presence of each compound at the indicated concentration, and in the flow cytometry results, the selected compounds **2j** and **4d** caused a markable increase in the percentage of cells blocked in the G2-M phase of the cell cycle (37% and 41%, respectively), with a simultaneous decrease of cells in S and G0-G1 phases, which was stronger than the effect of MT-7 (Fig. 1).¹⁴ These data suggested that this class of molecules inhibited the proliferation of HeLa cells through cell cycle arrest.

2.3. In vitro tubulin polymerization and colchicine site binding assays

It has been well documented that microtubule inhibitors preferentially arrest cells at the G2/M phase, so we investigated whether microtubule system could be a potential target of these compounds.^{17–19} Compounds **2j** and **4a–h** were evaluated for their direct inhibitory effects on tubulin polymerization in vitro, as presented in Figure 2A. Purified tubulins were polymerized to steady state in the presence of GTP at 37 °C in a control sample and as expected, treatment with these compounds inhibited tubulin

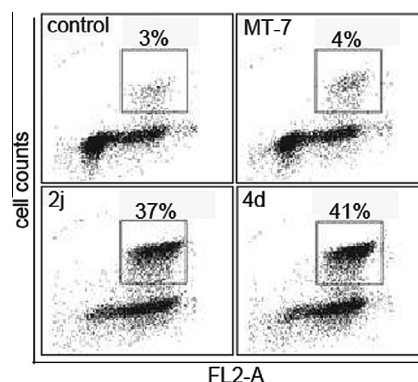


Figure 1. Cell cycle distribution of HeLa cells was analysed after treatment of 0.5 μM MT7, **2j** and **4d**.

polymerization to varying degrees consistent with their in vitro antiproliferative activity (Fig. 2B). Further analysis revealed that compounds **2j** (76%) and **4d** (74%) were as active as the reference inhibitor 20 μ M VCR (77%) and 20 μ M colchicines (76%), although both compounds were less active in their effects on cell proliferation. To evaluate if the compounds interacted with tubulin at the colchicine site, we determined whether **2j** and **4a–h** inhibited binding of 5 μ M [³H]-colchicine to 3 μ M tubulin. In the colchicine site binding studies, 20 μ M compounds **2j** and **4d**, with 74% and

78% inhibition, respectively, exhibited the ability to compete for the colchicine binding site about as potent as the positive reference inhibitor colchicine 77% (Fig. 2C). The colchicine site binding capacity for **2j** and **4a–h** may contribute to their antitubulin polymerization activity and further antiproliferative ability.

2.4. Disruption of mitotic spindle assembly

Proper tubulin polymerization is essential for the assembly of mitotic spindle, guaranteeing the precise segregation of chromosomes.^{20,1} Since these compounds could bind to the colchicine site to disrupt the polymerization of tubulin, we further examined their effect on the bipolar spindle formation. Immunofluorescence analysis was performed to evaluate the selected compounds **2j** and **4d** on the cellular mitotic spindle assembly. As shown in Figure 3A, the mitotic spindle exhibited normal bipolar orientation with chromosomes ordered alignment in HeLa cells without treatment. In contrast, 12 h of exposure to 0.5 μ M selected compounds caused multipolar mitotic spindle, with disordered chromosome organization. Then the percentage of cells with abnormal spindle assembly in total mitotic cells was calculated. As expected, compounds **2j** and **4d** disrupting mitotic spindle assembly in accordance with their anti-proliferation and anti-tubulin activities (Fig. 3B).

3. Conclusion

We have presented a series of 6*H*-pyrido[2',1':2,3]imidazo[4,5-*c*]isoquinolin-5(6*H*)-ones compounds, in which **2j** and **4a–h** exerted antiproliferative activity and proved as inhibitors of tubulin polymerization through binding to colchicine site. Selected compounds **2j** and **4d** were efficacious inhibiting tumor cell proliferation with IC₅₀ values at the low nanomolar level. Our studies revealed that a 4-methoxy substitution pattern in the terminal phenyl ring is critical for strong inhibition of tumor cell proliferation and inhibition of tubulin polymerization. The compounds described in this report are structurally simpler than the well-known colchicine or combretastatin A-4, chemically stable, and easily accessible.²¹ Due to their promising in vitro antiproliferative activities, we believe that the compounds of this structural class are attractive for further structural modifications and may provide a useful template for the design of new antitumoral agents. Structure–activity relationship studies concerning the pharmacophore requirements for activity are in progress and will be reported in due course.

4. Experimental section

4.1. Chemistry

4.1.1. General methods

Reagents were purchased from Aldrich or Lancaster and were used as received, isocyanides were purchased or prepared according to the procedure reported in the literature. The solvents were not dried prior to use. Melting points were determined in open capillary tubes on an Electrothermal melting point apparatus and are uncorrected. ¹H (300 MHz) and ¹³C NMR (100 MHz) spectra were measured at 25 °C on compounds in solution in CDCl₃ or DMSO-*d*₆ on a Varian spectrometer. Chemical shifts (δ) are given in ppm downfield from tetramethylsilane, an internal standard. The following abbreviations were used to explain the multiplicities: s = singlet, d = doublet, t = triplet, q = quartet, dd = doublet of doublets, m = multiplet, br = broad. The high resolution mass spectra were measured on Finnigan MAT 95 and MicroMass Q-ToF ultima™ mass spectrometers. Microwave reaction was conducted with a Biotage microwave reactor.

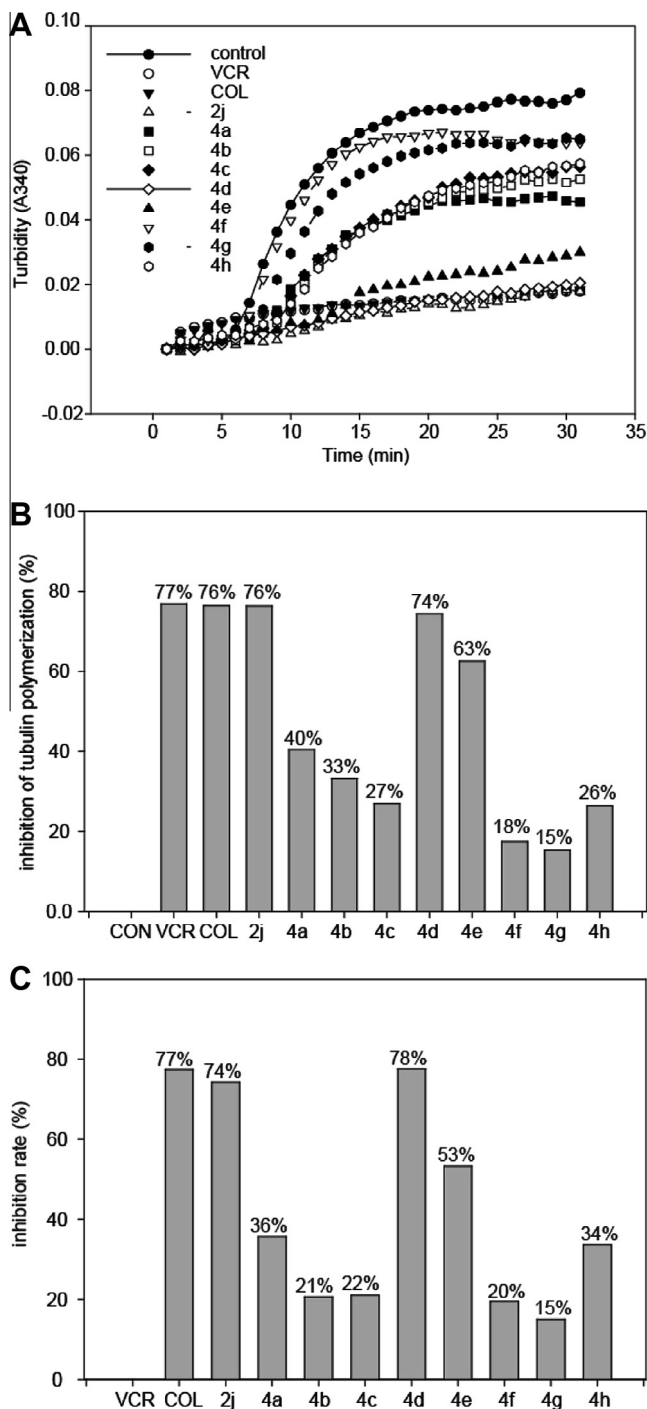


Figure 2. (A) The inhibitory activity of **2j** and **4a–h** against tubulin polymerization was examined in a cell-free system; (B) The inhibition percent of tubulin polymerization for **2j** and **4a–h** in the above cell-free system; (C) The capacities of **2j** and **4a–h** to bind to the colchicine site on tubulins were evaluated by site competitive binding assays.

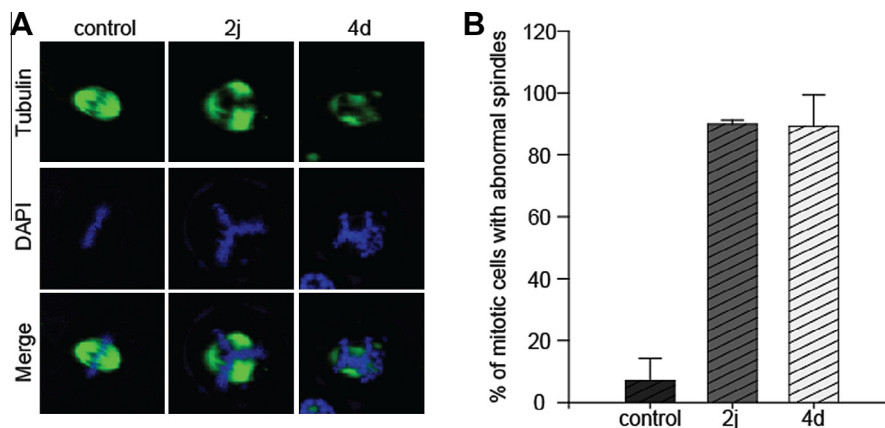


Figure 3. (A) Immunofluorescent microscope was used to observe the spindle assembly after treatment with compounds for 12 h; (B) The number of cells with the disorganized spindle was calculated in each sample.

4.1.2. General procedure a for synthesis of compounds 1c–1f and 2a–2j and 2l

To a mixture of 2-formylbenzoic acid (100 mg, 0.67 mmol), 2-amino-pyridine type amine (1 equiv) in MeOH (1 mL) was added with isocyanide (1 equiv). The reaction mixture was stirred at 55 °C and monitored by TLC, typically the reaction time is 4–12 h. After the reaction was completed, the precipitate that formed was isolated by filtration and washed with MeOH (1 mL × 3) to give the desired product.

4.1.2.1. 6-(4-Methoxybenzyl)-8-methylpyrido[2',1':2,3]imidazo[4,5-c]isoquinolin-5(6H)-one (1c). Yellow solid (72% yield, HPLC purity: 96.7); mp 146–148 °C; ¹H NMR (300 MHz, CDCl₃) δ 8.37(d, *J* = 5.1 Hz, 1H), 8.35(d, *J* = 5.1 Hz, 1H), 7.78(m, 1H), 7.55(d, *J* = 9.2 Hz, 1H), 7.49(t, *J* = 7.1 Hz, 1H), 7.13(dd, *J* = 9.2, 7.0 Hz, 1H), 6.81–6.84(m, 2H), 6.61–6.65(m, 3H), 5.47(s, 2H), 3.66(s, 3H), 2.93(s, 3H); HRMS(EI) *m/z* calcd for C₂₃H₁₉N₃O₂, 369.1477; found, 369.1480.

4.1.2.2. 6-(4-Methoxybenzyl)-11-methylpyrido[2',1':2,3]imidazo[4,5-c]isoquinolin-5(6H)-one (1d). Yellow solid (70% yield, HPLC purity: 98.6); mp 197–200 °C; ¹H NMR (300 MHz, CDCl₃) δ 8.58(d, *J* = 5.1 Hz, 1H), 8.55(d, *J* = 5.1 Hz, 1H), 8.10(d, *J* = 7.3 Hz, 1H), 7.85(t, *J* = 7.9 Hz, 1H), 7.59(t, *J* = 7.7 Hz, 1H), 7.16–7.18(m, 2H), 6.92(d, *J* = 7.0 Hz, 1H), 6.86–6.89(m, 2H), 6.56(t, *J* = 7.0 Hz, 1H), 5.85(s, 2H), 3.76(s, 3H), 2.69(s, 3H); HRMS(EI) *m/z* calcd for C₂₃H₁₉N₃O₂, 369.1477; found, 369.1480.

4.1.2.3. 9-Bromo-6-(4-methoxybenzyl)-8-methylpyrido[2',1':2,3]imidazo[4,5-c]isoquinolin-5(6H)-one (1e). Yellow solid (49% yield, HPLC purity: 100); mp 205–207 °C; ¹H NMR (300 MHz, CDCl₃) δ 8.12(d, *J* = 8.1 Hz, 1H), 7.50(t, *J* = 7.7 Hz, 1H), 7.43(d, *J* = 8.8 Hz, 1H), 7.12–7.22(m, 4H), 7.07(d, *J* = 7.7 Hz, 1H), 6.82–6.85(m, 2H), 4.47(d, *J* = 6.2 Hz, 2H), 3.79(s, 3H), 2.53(s, 3H); HRMS(EI) *m/z* calcd for C₂₃H₁₈BrN₃O₂, 447.0582; found, 447.0580.

4.1.2.4. 9-Bromo-6-(4-methoxybenzyl)-10-methylpyrido[2',1':2,3]imidazo[4,5-c]isoquinolin-5(6H)-one (1f). Yellow solid (50% yield, HPLC purity: 96.5); mp 197–200 °C; ¹H NMR (300 MHz, CDCl₃) δ 8.56(d, *J* = 8.1 Hz, 1H), 8.45(s, 1H), 8.41(d, *J* = 7.3 Hz, 1H), 7.85(m, 1H), 7.60(t, *J* = 7.5 Hz, 1H), 7.47(s, 1H), 7.17–7.20(m, 2H), 6.88–6.91(m, 2H), 5.83(s, 2H), 3.77(s, 3H), 2.38(s, 3H); HRMS(EI) *m/z* calcd for C₂₃H₁₈BrN₃O₂, 447.0582; found, 447.0579.

4.1.2.5. Methyl (5-oxopyrido[2',1':2,3]imidazo[4,5-c]isoquinolin-6(5H)-yl)acetate (2a). Yellow solid (67% yield, HPLC purity: 100); mp 212–214 °C; ¹H NMR (300 MHz, CDCl₃) δ 8.51(d, *J* = 8.1 Hz, 1H), 8.46(d, *J* = 7.3 Hz, 1H), 8.19(d, *J* = 8.1 Hz, 1H), 7.85(t, *J* = 7.7 Hz, 1H), 7.45(d, *J* = 9.2 Hz, 1H), 7.59(t, *J* = 7.5 Hz, 1H), 7.20(dd, *J* = 9.3, 6.8 Hz, 1H), 6.86(t, *J* = 7.0 Hz, 1H), 5.50(s, 2H), 3.84(s, 3H); HRMS(EI) *m/z* calcd for C₁₇H₁₃N₃O₃, 307.0957; found, 307.0960.

4.1.2.6. Methyl 3-(5-oxopyrido[2',1':2,3]imidazo[4,5-c]isoquinolin-6(5H)-yl)propanoate (2b). Yellow solid (60% yield, HPLC purity: 96.7); mp 205–207 °C; ¹H NMR (300 MHz, CDCl₃) δ 8.57(t, *J* = 7.9 Hz, 1H), 8.48(t, *J* = 7.0 Hz, 1H), 8.42(t, *J* = 7.7 Hz, 1H), 7.82(m, 1H), 7.73(t, *J* = 9.2 Hz, 1H), 7.57(m, 1H), 7.20(m, 1H), 6.89(m, 1H), 4.94(t, *J* = 8.1 Hz, 2H), 3.76(s, 3H), 3.03(t, *J* = 8.1 Hz, 2H); HRMS(EI) *m/z* calcd for C₁₈H₁₅N₃O₃, 321.1113; found, 321.1111.

4.1.2.7. 2-(5-Oxopyrido[2',1':2,3]imidazo[4,5-c]isoquinolin-6(5H)-yl)ethyl acetate (2c). Yellow solid (55% yield, HPLC purity: 99.0); mp 247–250 °C; ¹H NMR (300 MHz, CDCl₃) δ 8.80(d, *J* = 7.3 Hz, 1H), 8.49(d, *J* = 8.4 Hz, 1H), 8.42(d, *J* = 8.1 Hz, 1H), 7.82(t, *J* = 7.7 Hz, 1H), 7.71(d, *J* = 9.5 Hz, 1H), 7.57(t, *J* = 7.7 Hz, 1H), 7.20(dd, *J* = 9.2, 6.6 Hz, 1H), 6.90(t, *J* = 7.0 Hz, 1H), 4.87(t, *J* = 6.6 Hz, 2H), 4.58(t, *J* = 6.6 Hz, 2H), 1.97(s, 3H); HRMS(EI) *m/z* calcd for C₁₈H₁₅N₃O₃, 321.1113; found, 321.1110.

4.1.2.8. 6-(2-Furylmethyl)pyrido[2',1':2,3]imidazo[4,5-c]isoquinolin-5(6H)-one (2d). Yellow solid (42% yield, HPLC purity: 98.1); mp 206–209 °C; ¹H NMR (300 MHz, CDCl₃) δ 8.55(d, *J* = 7.4 Hz, 1H), 8.51(d, *J* = 8.5 Hz, 1H), 8.42(d, *J* = 8.0 Hz, 1H), 7.82(t, *J* = 7.6 Hz, 1H), 7.68(d, *J* = 9.1 Hz, 1H), 7.56(t, *J* = 7.7 Hz, 1H), 7.39(s, 1H), 7.16(dd, *J* = 8.9, 6.7 Hz, 1H), 6.79(t, *J* = 6.9 Hz, 1H), 6.34–6.40(m, 2H), 5.83(s, 2H); ¹³C NMR (100 MHz, CDCl₃) δ_c: 161.41, 149.00, 143.12, 142.69, 133.27, 131.81, 129.36, 127.20, 125.17, 124.23, 123.86, 123.76, 123.52, 121.93, 118.72, 112.48, 111.00, 109.07, 40.54. HRMS(EI) *m/z* calcd for C₁₉H₁₃N₃O₂, 315.1008; found, 315.1010.

4.1.2.9. 6-[4-(Trifluoromethoxy)benzyl]pyrido[2',1':2,3]imidazo[4,5-c]isoquinolin-5(6H)-one (2e). Yellow solid (56% yield, HPLC purity: 99.1); mp 220–222 °C; ¹H NMR (300 MHz, CDCl₃) δ 8.53(d, *J* = 8.3 Hz, 1H), 8.45(d, *J* = 8.0 Hz, 1H), 8.08(d, *J* = 7.2 Hz, 1H), 7.85(m, 1H), 7.66(d, *J* = 9.4 Hz, 1H), 7.59(m, 1H), 7.20–7.32(m, 4H), 7.09(m, 1H), 6.63(m, 1H), 5.89(s, 2H); ¹³C NMR (100 MHz, CDCl₃) δ_c: 161.66, 148.78, 143.02, 134.65, 133.41,

131.88, 129.48, 127.33, 127.06 × 3, 125.19, 124.30, 123.77 × 2, 122.67, 121.96, 121.89 × 2, 118.85, 112.77, 46.28; HRMS(EI) *m/z* calcd for C₂₂H₁₄F₃N₃O₂, 409.1038; found, 409.1034.

4.1.2.10. 6-(3,4-Dimethoxybenzyl)pyrido[2,1':2,3]imidazo[4,5-c]isoquinolin-5(6H)-one (2f). Yellow solid (44% yield, HPLC purity: 100); mp 180–183 °C; ¹H NMR (300 MHz, CDCl₃) δ 8.55(d, *J* = 7.9 Hz, 1H), 8.45(d, *J* = 7.6 Hz, 1H), 8.18(d, *J* = 7.3 Hz, 1H), 7.85(t, *J* = 7.6 Hz, 1H), 7.65(d, *J* = 9.2 Hz, 1H), 7.59(t, *J* = 7.8 Hz, 1H), 7.09(m, 1H), 6.70–6.83(m, 3H), 6.61(t, *J* = 6.6 Hz, 1H), 5.84(s, 2H), 3.83(s, 3H), 3.82(s, 3H); ¹³C NMR (100 MHz, CDCl₃) δ_c: 161.52, 149.65, 148.53, 142.85, 133.12, 131.62, 129.31, 128.17, 127.07, 124.75, 124.53, 123.74, 123.22, 121.75, 118.36, 117.36, 112.43, 111.64, 108.60, 55.88, 55.75, 50.40, 46.45; HRMS(EI) *m/z* calcd for C₂₃H₁₉N₃O₃, 385.1426; found, 385.1422.

4.1.2.11. 6-(2,4-Dimethoxybenzyl)pyrido[2,1':2,3]imidazo[4,5-c]isoquinolin-5(6H)-one (2g). Yellow solid (58% yield, HPLC purity: 96.3); mp 188–200 °C; ¹H NMR (300 MHz, CDCl₃) δ 8.56(d, *J* = 7.4 Hz, 1H), 8.45(d, *J* = 8.0 Hz, 1H), 8.12(d, *J* = 7.4 Hz, 1H), 7.83(m, 1H), 7.55–7.63(m, 2H), 7.06(ddd, *J* = 9.2, 6.6, 1.0 Hz, 1H), 6.78(d, *J* = 8.5 Hz, 1H), 6.55–6.59(m, 2H), 6.30(dd, *J* = 8.5, 2.2 Hz, 1H), 5.77(s, 2H), 3.95(s, 3H), 3.73(s, 3H); ¹³C NMR (100 MHz, CDCl₃) δ_c: 161.75, 160.54, 156.69, 143.05, 133.08, 131.84, 129.49, 127.07, 127.04, 125.02, 124.76, 124.03, 123.64, 123.45, 121.85, 118.46, 116.19, 112.30, 104.62, 98.88, 55.54, 55.33, 41.92; HRMS(EI) *m/z* calcd for C₂₃H₁₉N₃O₃, 385.1426; found, 385.1426.

4.1.2.12. 6-(1,3-Benzodioxol-5-ylmethyl)pyrido[2,1':2,3]imidazo[4,5-c]isoquinolin-5(6H)-one (2h). Yellow solid (67% yield, HPLC purity: 100); mp 216–219 °C; ¹H NMR (300 MHz, CDCl₃) δ 8.52(d, *J* = 8.3 Hz, 1H), 8.42(d, *J* = 8.0 Hz, 1H), 8.17(d, *J* = 7.2 Hz, 1H), 7.83(m, 1H), 7.62(d, *J* = 9.1 Hz, 1H), 7.57(m, 1H), 7.07(ddd, *J* = 9.2, 6.7, 1.1 Hz, 1H), 6.68–6.76(m, 3H), 6.61(m, 1H), 5.92(s, 2H), 5.79(s, 2H); ¹³C NMR (100 MHz, CDCl₃) δ_c: 161.61, 148.62, 147.25, 142.98, 133.24, 131.83, 129.62, 129.47, 127.19, 125.06, 124.53, 123.87, 123.70, 123.20, 121.88, 118.64, 118.56, 112.55, 108.96, 106.06, 101.26, 46.51; HRMS(EI) *m/z* calcd for C₂₂H₁₅N₃O₃, 369.1113; found, 369.1116.

4.1.2.13. N-Methyl-N-[4-[(5-oxopyrido[2,1':2,3]imidazo[4,5-c]isoquinolin-6(5H)-yl)methyl]phenyl]methanesulfonamide (2i). Yellow solid (34% yield, HPLC purity: 96.7); mp 233–236 °C; ¹H NMR (300 MHz, DMSO-*d*₆) δ 8.33–8.41(m, 3H), 7.91(t, *J* = 7.5 Hz, 1H), 7.60–7.67(m, 2H), 7.29–7.40(m, 4H), 7.20(dd, *J* = 9.1, 6.7 Hz, 1H), 6.82(t, *J* = 6.9 Hz, 1H), 5.98(s, 2H), 3.19(s, 3H), 2.91(s, 3H); ¹³C NMR (100 MHz, DMSO-*d*₆) δ_c: 160.55, 142.35, 140.83, 135.36, 133.29, 131.65, 128.91, 127.07, 126.69 × 2, 126.42 × 2, 124.45, 124.16, 124.03, 123.35, 121.64, 118.01, 112.41, 45.28, 37.63, 35.02; HRMS(EI) *m/z* calcd for C₂₃H₂₀N₄O₃S, 432.1256; found, 432.1261.

4.1.2.14. 6-[2-(4-Methoxyphenyl)ethyl]pyrido[2,1':2,3]imidazo[4,5-c]isoquinolin-5(6H)-one (2j). Yellow solid (67% yield, HPLC purity: 96.5); mp 155–157 °C; ¹H NMR (300 MHz, CDCl₃) δ 8.48(d, *J* = 8.3 Hz, 1H), 8.39(d, *J* = 7.7 Hz, 1H), 8.35(d, *J* = 7.2 Hz, 1H), 7.79(m, 1H), 7.68(d, *J* = 9.4 Hz, 1H), 7.55(m, 1H), 7.21–7.27(m, 2H), 7.15(ddd, *J* = 9.3, 6.7, 1.1 Hz, 1H), 6.85–6.88(m, 2H), 6.81(m, 1H), 4.80(t, *J* = 8.0 Hz, 2H), 3.78(s, 3H), 3.15(t, *J* = 8.0 Hz, 2H); ¹³C NMR (100 MHz, CDCl₃) δ_c: 161.24, 158.65, 142.90, 132.96, 131.55, 129.63 × 2, 129.11, 129.07, 127.11, 125.10, 124.29, 124.01, 123.41, 122.58, 121.82, 119.00, 114.29 × 2, 112.75, 55.25, 44.45, 34.86; HRMS(EI) *m/z* calcd for C₂₃H₁₉N₃O₂, 369.1477; found, 369.1479.

4.1.2.15. 6-[3-(4-Methoxyphenyl)propyl]pyrido[2,1':2,3]imidazo[4,5-c]isoquinolin-5(6H)-one (2l). Yellow solid (61% yield, HPLC purity: 99.5); mp 170–173 °C; ¹H NMR (300 MHz, CDCl₃) δ 8.43(d, *J* = 8.0 Hz, 1H), 8.31(d, *J* = 7.4 Hz, 1H), 7.73(t, *J* = 8.3 Hz, 1H), 7.47–7.60(m, 3H), 7.18(d, *J* = 8.4 Hz, 2H), 7.01(m, 1H), 6.89(d, *J* = 8.4 Hz, 2H), 6.41(m, 1H), 4.40(t, *J* = 8.1 Hz, 2H), 3.82(s, 3H), 2.81(t, *J* = 8.1 Hz, 2H), 2.17(m, 2H); ¹³C NMR (100 MHz, CDCl₃) δ_c: 161.11, 158.13, 142.70, 132.71, 132.26, 131.34, 129.68 × 2, 128.96, 126.88, 124.73, 124.13, 123.78, 123.29, 122.72, 121.64, 118.57, 114.00 × 2, 112.36, 55.24, 42.25, 31.93, 31.13; HRMS(EI) *m/z* calcd for C₂₄H₂₁N₃O₂, 383.1634; found, 383.1626.

4.1.2.16. 6-[2-(4-Hydroxyphenyl)ethyl]pyrido[2,1':2,3]imidazo[4,5-c]isoquinolin-5(6H)-one (2k). To a stirred solution of compound **2j** (50 mg, 0.2 mmol) in 4 mL of dry dichloromethane was added at –78 °C a solution of 0.04 mL (0.4 mmol) of BBr₃ in 1 mL of dichloromethane. After 1 h the mixture was warmed to –25 °C. The reaction was monitored by TLC, after completion, the mixture was quenched with saturated sodium hydrogen carbonate. The usual workup yielded 41 mg of the pure product as yellow solid (yield 85%, HPLC purity: 98.6), mp 280–283 °C; ¹H NMR (300 MHz, DMSO-*d*₆) δ 9.16(s, 1H), 8.51(d, *J* = 7.0 Hz, 1H), 8.21(d, *J* = 7.9 Hz, 1H), 8.17(d, *J* = 7.9 Hz, 1H), 7.74(t, *J* = 7.3 Hz, 1H), 7.57(d, *J* = 9.2 Hz, 1H), 7.47(t, *J* = 7.5 Hz, 1H), 7.18(m, 1H), 6.87–6.96(m, 2H), 6.56(d, *J* = 8.2 Hz, 2H), 4.70(t, *J* = 7.3 Hz, 2H), 2.86(t, *J* = 7.3 Hz, 2H); ¹³C NMR (100 MHz, DMSO-*d*₆) δ_c: 160.11, 156.04, 142.29, 132.91, 131.30, 129.65 × 2, 128.66, 127.55, 126.84, 124.36, 124.22, 124.05, 123.76, 123.42, 121.47, 118.01, 115.28 × 2, 112.58, 43.69, 34.22. ESI: *m/z* (relative intensity) 356.1(M+1, 100%).

4.1.3. General procedure B (Ullmann coupling) for synthesis of compounds 4a–4h

In a 10 mL Biotage vial was charged with the compound **3** (1 equiv, prepared according to the procedure A), the appropriate amines (10 equiv), copper(I) iodide (0.15 equiv), *L*-proline (0.2 equiv), potassium carbonate (2.0 equiv) and 4 mL of DMSO. The vial was sealed with a septum and the resulting suspension was heated in the Biotage Initiator Synthesizer under 150 °C (300 W) over 10 min. The reaction mixture was cooled to ambient temperature, and evaporated in vacuo. The residue was dissolved with CH₂Cl₂ (30 mL), and the resultant solution was washed sequentially with water (10 mL), and brine (10 mL). The organic layer was dried, filtered, and evaporated, and the residue was purified by flash chromatography on silica gel (CH₂Cl₂/MeOH = 10:1) to afford the desired products.

4.1.3.1. 9-(1H-Imidazol-1-yl)-6-[2-(4-methoxyphenyl)ethyl]pyrido[2,1':2,3]imidazo[4,5-c]isoquinolin-5(6H)-one (4a). Brown solid (61% yield, HPLC purity: 96.8); mp 240–244 °C; ¹H NMR (300 MHz, CDCl₃) δ 8.53(d, *J* = 8.3 Hz, 1H), 8.42(d, *J* = 8.0 Hz, 1H), 8.29(s, 1H), 7.85(m, 1H), 7.75–7.79(d, *J* = 9.6 Hz, 2H), 7.62(m, 1H), 7.31(br s, 1H), 7.21(dd, *J* = 9.6, 1.9 Hz, 2H), 7.07(d, *J* = 8.5 Hz, 2H), 6.71(d, *J* = 8.5 Hz, 2H), 4.80(t, *J* = 7.5 Hz, 2H), 3.73(s, 3H), 3.22(t, *J* = 7.5 Hz, 2H); ¹³C NMR (100 MHz, CDCl₃) δ_c: 161.40, 158.84, 141.35, 133.34, 131.32, 131.06, 129.54 × 3, 129.32, 128.92, 127.79, 126.69, 125.70, 125.24, 124.28, 122.01, 119.84, 119.64, 116.48, 114.50 × 3, 55.27, 44.90, 34.88; HRMS(EI) *m/z* calcd for C₂₆H₂₁N₅O₂, 435.1695; found, 435.1697.

4.1.3.2. 9-[[3-(1H-Imidazol-1-yl)propyl]amino]-6-[2-(4-methoxyphenyl)ethyl]pyrido[2,1':2,3]imidazo[4,5-c]isoquinolin-5(6H)-one (4b). Brown solid (70% yield, HPLC purity: 100); mp 180–182 °C; ¹H NMR (300 MHz, CDCl₃) δ 8.49(d, *J* = 7.6 Hz, 1H), 8.36(d, *J* = 7.9 Hz, 1H), 7.78(t, *J* = 7.5 Hz, 1H), 7.48–7.56(m, 3H), 7.39(s, 1H), 7.21(d, *J* = 9.0 Hz, 2H), 7.09(s, 1H), 6.84–6.88(m,

3H), 6.7(dd, $J = 9.8, 1.5$ Hz, 1H), 4.86(m, 2H), 4.01(t, $J = 6.9$ Hz, 2H), 3.79(s, 3H), 3.22(m, 2H), 2.82(t, $J = 6.6$ Hz, 2H), 1.26(m, 2H); ^{13}C NMR (100 MHz, CDCl_3) δ_{C} : 161.45, 158.70, 140.19, 136.18, 132.97, 131.97, 129.5 \times 5, 129.20, 126.74, 124.91, 123.74, 121.58, 119.50, 119.11, 118.71, 114.29 \times 3, 101.67, 55.36, 44.39, 43.73, 41.12, 34.71, 30.33; HRMS(EI) m/z calcd for $\text{C}_{29}\text{H}_{28}\text{N}_6\text{O}_2$, 492.2274; found, 492.2275.

4.1.3.3. 6-[2-(4-Methoxyphenyl)ethyl]-9-[(pyridin-2-ylmethyl)amino]pyrido[2,1':2,3]imidazo[4,5-c]isoquinolin-5(6H)-one

(4c). Brown solid (52% yield, HPLC purity: 96.9); mp 190–193 °C; ^1H NMR (300 MHz, CDCl_3) δ 8.57(d, $J = 4.9$ Hz, 1H), 8.47(d, $J = 7.6$ Hz, 1H), 8.35(d, $J = 7.9$ Hz, 1H), 7.75(m, 1H), 7.67(td, $J = 7.8, 1.8$ Hz, 1H), 7.47–7.55(m, 3H), 7.27–7.30(m, 2H), 7.22(dd, $J = 7.0, 5.5$ Hz, 1H), 7.13(d, $J = 7.9$ Hz, 1H), 6.86–6.89(m, 3H), 4.86(m, 2H), 4.14(s, 2H), 3.78(s, 3H), 3.20(m, 2H); ^{13}C NMR (100 MHz, $\text{DMSO}-d_6$) δ_{C} : 161.39, 158.57, 156.07, 149.12, 140.14, 136.72, 136.29, 132.84, 131.94, 129.63 \times 2, 129.47, 129.11, 126.54, 124.95, 124.82, 123.63, 122.57, 121.89, 121.48, 119.94, 118.82, 114.18 \times 2, 101.51, 55.24, 48.84, 43.80, 34.83; HRMS(EI) m/z calcd for $\text{C}_{29}\text{H}_{25}\text{N}_5\text{O}_2$, 475.2008; found, 475.2026.

4.1.3.4. 6-[2-(4-Methoxyphenyl)ethyl]-9-[(pyridin-3-ylmethyl)amino]pyrido[2,1':2,3]imidazo[4,5-c]isoquinolin-5(6H)-one

(4d). Brown solid (58% yield, HPLC purity: 96.7); mp 188–190 °C; ^1H NMR (300 MHz, $\text{DMSO}-d_6$) δ 8.44–8.45(m, 3H), 8.34(d, $J = 8.0$ Hz, 1H), 7.76(t, $J = 7.4$ Hz, 1H), 7.48–7.56(m, 3H), 7.40(s, 1H), 7.26(m, 1H), 7.16–7.19(d, $J = 8.5$ Hz, 2H), 6.78–6.83(m, 3H), 4.76(t, $J = 8.0$ Hz, 2H), 3.71(s, 3H), 3.12(t, $J = 8.0$ Hz, 2H); ^{13}C NMR (100 MHz, CDCl_3) δ_{C} : 161.29, 158.62, 149.17, 148.98, 140.08, 135.87, 135.18, 133.08, 132.90, 131.79, 129.43 \times 3, 129.14, 126.66, 125.05, 124.76, 123.60, 121.47, 119.51, 118.99, 114.17 \times 3, 101.88, 55.19, 45.90, 40.90, 34.64; HRMS(EI) m/z calcd for $\text{C}_{29}\text{H}_{25}\text{N}_5\text{O}_2$, 475.2008; found, 475.2010.

4.1.3.5. 6-[2-(4-Methoxyphenyl)ethyl]-9-[(pyridin-4-ylmethyl)amino]pyrido[2,1':2,3]imidazo[4,5-c]isoquinolin-5(6H)-one

(4e). Brown amorphous solid (56% yield, HPLC purity: 100); ^1H NMR (300 MHz, $\text{DMSO}-d_6$) δ 8.17–8.24(m, 3H), 7.75–7.80(m, 2H), 7.46–7.53(m, 3H), 7.34(s, 1H), 6.99–7.06(m, 3H), 6.75–6.78(d, $J = 8.2$ Hz, 2H), 6.42(t, $J = 6.5$ Hz, 1H), 4.67(t, $J = 7.3$ Hz, 2H), 4.23(s, 2H), 3.66(s, 3H), 2.81(t, $J = 7.3$ Hz, 2H); ^{13}C NMR (100 MHz, $\text{DMSO}-d_6$) δ_{C} : 160.24, 158.00, 149.66, 148.01, 139.39, 136.39, 132.92, 131.71, 129.48 \times 4, 129.28, 128.72, 126.34, 124.51, 123.68, 122.96, 121.16, 120.28, 118.22, 113.87 \times 3, 100.98, 55.03, 45.84, 42.94, 34.13; HRMS(EI) m/z calcd for $\text{C}_{29}\text{H}_{25}\text{N}_5\text{O}_2$, 475.2008; found, 475.2010.

4.1.3.6. 9-[[2-(Diethylamino)ethyl]amino]-6-[2-(4-methoxyphenyl)ethyl]pyrido[2,1':2,3]imidazo[4,5-c]isoquinolin-5(6H)-one

(4f). Brown amorphous solid (71% yield, HPLC purity: 98.3); ^1H NMR (300 MHz, $\text{DMSO}-d_6$) δ 8.31(d, $J = 8.2$ Hz, 1H), 8.23(d, $J = 7.9$ Hz, 1H), 7.83(m, 1H), 7.47–7.64(m, 3H), 7.21–7.26(m, 2H), 7.01(d, $J = 9.8$ Hz, 1H), 6.84–6.89(m, 2H), 4.84(m, 2H), 4.49(m, 2H), 3.72(s, 3H), 2.89–3.09(m, 4H), 2.73(m, 2H), 2.60(m, 2H), 1.07(m, 6H); ^{13}C NMR (100 MHz, $\text{DMSO}-d_6$) δ_{C} : 160.30, 158.06, 139.43, 136.95, 132.88, 131.81, 129.45 \times 2, 129.36, 128.67, 126.25, 124.57, 123.56, 122.95, 121.11, 120.59, 117.89, 113.98 \times 2, 100.33, 55.01, 50.82, 46.41 \times 2, 43.34, 41.11, 34.46, 11.20 \times 2; HRMS(EI) m/z calcd for $\text{C}_{29}\text{H}_{33}\text{N}_5\text{O}_2$, 483.2634; found, 483.2632.

4.1.3.7. 6-[2-(4-Methoxyphenyl)ethyl]-9-[(2-morpholin-4-ylethyl)amino]pyrido[2,1':2,3]imidazo[4,5-c]isoquinolin-5(6H)-one

(4g). Brown amorphous solid (68% yield, HPLC purity: 98.8); ^1H NMR (300 MHz, $\text{DMSO}-d_6$) δ 8.32(d, $J = 7.6$ Hz, 1H), 8.24(d,

$J = 7.0$ Hz, 1H), 7.84(m, 1H), 7.49–7.57(m, 3H), 7.25(d, $J = 8.6$ Hz, 2H), 7.02(m, 1H), 6.87–6.90(m, 2H), 4.88(m, 2H), 3.74(s, 3H), 3.59(m, 3H), 3.00–3.14(m, 6H), 2.41(m, 3H); ^{13}C NMR (100 MHz, $\text{DMSO}-d_6$) δ_{C} : 160.21, 158.00, 139.34, 136.88, 132.82, 131.80, 129.40 \times 3, 128.63, 126.16, 123.50, 122.90, 121.04, 120.54, 117.86, 113.93 \times 3, 100.12, 65.99 \times 3, 54.98, 53.21 \times 2, 43.22, 34.40 \times 2; HRMS(EI) m/z calcd for $\text{C}_{29}\text{H}_{31}\text{N}_5\text{O}_3$, 497.2427; found, 497.2418.

4.1.3.8. 9-[(2-Hydroxyethyl)amino]-6-[2-(4-methoxyphenyl)ethyl]pyrido[2,1':2,3]imidazo[4,5-c]isoquinolin-5(6H)-one

(4h). Brown amorphous solid (80% yield, HPLC purity: 99.1); ^1H NMR (300 MHz, $\text{DMSO}-d_6$) δ 8.24(d, $J = 7.9$ Hz, 1H), 8.16(d, $J = 7.9$ Hz, 1H), 7.74(t, $J = 7.5$ Hz, 1H), 7.39–7.48(m, 3H), 7.18(d, $J = 8.5$ Hz, 2H), 6.98(d, $J = 9.7$ Hz, 1H), 6.84(d, $J = 8.5$ Hz, 2H), 5.61(br s, 1H), 4.85(br s, 1H), 4.72(t, $J = 7.8$ Hz, 2H), 3.70(s, 3H), 3.62(t, $J = 4.8$ Hz, 2H), 2.95–3.04(m, 4H); ^{13}C NMR (100 MHz, $\text{DMSO}-d_6$) δ_{C} : 160.20, 158.05, 139.33, 137.19, 132.74, 131.75, 129.52 \times 2, 129.40, 128.61, 126.12, 124.49, 123.44, 122.88, 121.06, 120.60, 117.80, 113.99 \times 2, 99.87, 59.39, 55.03, 46.11, 43.49, 34.52; HRMS(EI) m/z calcd for $\text{C}_{25}\text{H}_{24}\text{N}_4\text{O}_3$, 428.1844; found, 428.1844.

4.2. Sulforhodamine B (SRB) assays

HeLa cells were purchased from the American Type Culture Collection (Manassas, VA). HeLa cells were treated with indicated compounds for 72 h and then were fixed with 10% pre-cooled trichloroacetic acid (TCA), washed with distilled water, and stained with SRB (Sigma–Aldrich, St. Louis, MO) in 1% acetic acid. SRB in the cells was dissolved in 10 mM Tris–HCl and was measured at 515 nm with spectraMAX190 (Molecular Devices, Sunnyvale, CA). The cell proliferation inhibition rate was calculated as: proliferation inhibition (%) = $[1 - (A_{515}^{\text{treated}}/A_{515}^{\text{control}})] \times 100\%$. The average IC_{50} values were determined with the Logit method from at least three independent tests.

4.3. In vitro tubulin polymerization assays

Purified tubulin was purchased from Cytoskeleton (Denver, CO, USA). 20 μM indicated compounds were mixed with tubulin in a 96-well plate on ice, respectively. The plate was put into a 37 °C incubator and tubulin polymerization was monitored at 340 nm with spectraMAX190 (Molecular Devices, Sunnyvale, CA). The reaction buffer for this assay contained 80 mM PIPES pH6.9, 0.5 mM EGTA, 2 mM MgCl_2 and 1 mM GTP.

4.4. Colchicine competitive binding assays

Tubulin (3 μM) was pre-incubated with 20 μM indicated compounds for 1 h, respectively, following which added [^3H]-colchicine (5 μM). After 30 min of incubation at 37 °C, the bound [^3H]-colchicine of each sample was determined using DE81 filter assays described by Gary G. Borisy.²²

4.5. Cell cycle progression analysis

HeLa cells were treated with 0.5 μM indicated compounds for 12 h, then harvested and washed with PBS, fixed with pre-cooled 70% ethanol at 4 °C. After being stained with 10 $\mu\text{g}/\text{ml}$ propidium iodide in the dark for 30 min, cells were collected with FACS Calibur (BD Biosciences, Franklin Lakes, NJ) and analysed by using the CELLQUEST software (BD Biosciences, Franklin Lakes, NJ).

4.6. Mitotic spindle assembly assays

After 0.5 μ M compounds treatments, HeLa cells cultured on glass coverslips were fixed with 4% paraformaldehyde, permeabilized with 0.2% TritonX-100 and saturated with 3% bovine serum albumin. Then the cells were incubated sequentially with the primary antibody against α -Tubulin (1:200, Invitrogen, Carlsbad, CA) and with Alexa FluorVR 488-conjugated goat anti-mouse IgG (1:100, Invitrogen, Carlsbad, CA) for 1 h, respectively. Finally, cells were stained with DAPI and imaged under an Olympus BX51 fluorescence microscope system (Olympus, Tokyo, Japan) and a Nikon Eclipse C1 Plus confocal microscope (Nikon, Tokyo, Japan).

Acknowledgments

This work was supported by the National Science & Technology Major Project 'Key New Drug Creation and Manufacturing Program', China (no.: 2012ZX09103-101-026).

Supplementary data

Supplementary data (copies of proton and carbon NMR for all the compounds) associated with this article can be found, in the online version, at <http://dx.doi.org/10.1016/j.bmc.2013.12.004>.

References and notes

- Jordan, A.; Hadfield, J. A.; Lawrence, N. J.; McGown, A. T. *Med. Res. Rev.* **1998**, *18*, 259.
- Abdullah, N. M.; Rosania, G. R.; Shedden, K. *PLoS One* **2009**, *4*, e4470.
- von Angerer, E. *Curr. Opin. Drug Disc.* **2000**, *3*, 575.
- Perez, E. A. *Mol. Cancer Ther.* **2009**, *8*, 2086.
- Kawaratan, Y.; Harada, T.; Hirata, Y.; Nagaoka, Y.; Tanimura, S.; Shibano, M.; Taniguchi, M.; Yasuda, M.; Baba, K.; Uesato, S. *Bioorg. Med. Chem.* **2011**, *19*, 3995.
- Carlson, R. O. *Expert Opin. Investig. Drugs* **2008**, *17*, 707.
- Hamel, E. *Med. Res. Rev.* **1996**, *16*, 207.
- For selected reviews, (a) Lu, Y.; Chen, J.; Xiao, M.; Li, W.; Miller, D. D. *Pharmacol. Res.* **2012**, *29*, 294; (b) Pellegrini, F.; Budman, D. R. *Cancer Invest.* **2005**, *23*, 264; (c) Chen, J.; Liu, T.; Dong, X.; Hu, Y. *Mini-Rev. Med. Chem.* **2009**, *9*, 1174.
- Owa, T.; Yokoi, A.; Yamazaki, K.; Yoshimatsu, K.; Yamori, T.; Nagasu, T. *J. Med. Chem.* **2002**, *45*, 4913.
- Flynn, B. L.; Gill, G. S.; Grobelny, D. W.; Chaplin, J. H.; Paul, D.; Leske, A. F.; Lavranos, T. C.; Chalmers, D. K.; Charman, S. A.; Kostewicz, E.; Shackelford, D. M.; Morizzi, J.; Hamel, E.; Jung, M. K.; Kremmidiotis, G. *J. Med. Chem.* **2011**, *54*, 6014.
- Risinger, A. L.; Westbrook, C. D.; Encinas, A.; Mulbaier, M.; Schultes, C. M.; Wawro, S.; Lewis, J. D.; Janssen, B.; Giles, F. J.; Mooberry, S. L. *J. Pharmacol. Exp. Ther.* **2011**, *336*, 652.
- Liberatore, A. M.; Coulomb, H.; Pons, D.; Dutruel, O.; Kasprzyk, P. G.; Carlson, M.; Nelson, A. S.; Newman, S. P.; Stengel, C.; Auvray, P.; Hesry, V.; Foll, B.; Narboux, N.; Morlais, D.; Le Moing, M.; Bernetiere, S.; Dellile, R.; Camara, J.; Ferrandis, E.; Bigg, D. C.; Prevost, G. P. *Mol. Cancer Ther.* **2008**, *7*, 2426.
- Meng, T.; Zhang, Z.; Hu, D.; Lin, L.; Ding, J.; Wang, X.; Shen, J. *J. Comb. Chem.* **2007**, *9*, 739.
- Zhang, Z.; Meng, T.; He, J.; Li, M.; Tong, L. J.; Xiong, B.; Lin, L.; Shen, J.; Miao, Z. H.; Ding, J. *Invest. New Drugs* **2010**, *28*, 715.
- Zhang, Z.; Meng, T.; Yang, N.; Wang, W.; Xiong, B.; Chen, Y.; Ma, L.; Shen, J.; Miao, Z. H.; Ding, J. *Int. J. Cancer* **2011**, *129*, 214.
- Viola, G.; Bortolozzi, R.; Hamel, E.; Moro, S.; Brun, P.; Castagliuolo, I.; Ferlin, M. G.; Basso, G. *Biochem. Pharmacol.* **2012**, *83*, 16.
- Li, C. M.; Wang, Z.; Lu, Y.; Ahn, S.; Narayanan, R.; Kearbey, J. D.; Parke, D. N.; Li, W.; Miller, D. D.; Dalton, J. T. *Cancer Res.* **2011**, *71*, 216.
- Arora, S.; Wang, X. I.; Keenan, S. M.; Andaya, C.; Zhang, Q.; Peng, Y.; Welsh, W. J. *Cancer Res.* **2009**, *69*, 1910.
- Qiao, F.; Zuo, D.; Wang, H.; Li, Z.; Qi, H.; Zhang, W.; Wu, Y. *Biol. Pharm. Bull.* **2013**, *36*, 193.
- Gomez-Ferrera, M. A.; Bashkurov, M.; Helbig, A. O.; Larsen, B.; Pawson, T.; Gingras, A. C.; Pelletier, L. *J. Cell Sci.* **2012**, *125*, 3745.
- Shen, J.K.; Meng, T.; Zhang, Z.X.; Miao, Z.H.; Ding, J.; Ma, L.P.; Hu, D.Y.; Zhang, Y.L.; Jin, Y.; Wang, X.; CN Patent 200810200953.7, 2008.
- Borisy, G. G.; Taylor, E. W. *J. Cell Biol.* **1967**, *34*, 525.